

Acta Crystallographica Section F

**Structural Biology
Communications**

ISSN 2053-230X

Purification, characterization and preliminary X-ray crystallographic studies of monodehydroascorbate reductase from *Oryza sativa* L. *japonica*

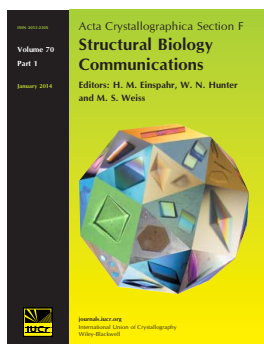
Hackwon Do, Il-Sup Kim, Young-Saeng Kim, Sun-Young Shin, Jin-Ju Kim, Ji-Eun Mok, Seong-Im Park, Ah Ram Wi, Hyun Park, Jun Hyuck Lee, Ho-Sung Yoon and Han-Woo Kim

Acta Cryst. (2014). **F70**, 1244–1248

Copyright © International Union of Crystallography

Author(s) of this paper may load this reprint on their own web site or institutional repository provided that this cover page is retained. Reproduction of this article or its storage in electronic databases other than as specified above is not permitted without prior permission in writing from the IUCr.

For further information see <http://journals.iucr.org/services/authorrights.html>



Acta Crystallographica Section F: Structural Biology Communications is a rapid all-electronic journal, which provides a home for short communications on the crystallization and structure of biological macromolecules. Structures determined through structural genomics initiatives or from iterative studies such as those used in the pharmaceutical industry are particularly welcomed. Articles are available online when ready, making publication as fast as possible, and include unlimited free colour illustrations, movies and other enhancements. The editorial process is completely electronic with respect to deposition, submission, refereeing and publication.

Crystallography Journals **Online** is available from journals.iucr.org

Purification, characterization and preliminary X-ray
crystallographic studies of monodehydroascorbate
reductase from *Oryza sativa* L. *japonica*

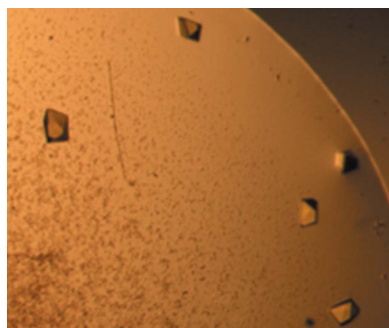
Hackwon Do,^{a,b} Il-Sup Kim,^c†
Young-Saeng Kim,^c Sun-Young
Shin,^c Jin-Ju Kim,^c Ji-Eun Mok,^c
Seong-Im Park,^c Ah Ram Wi,^a
Hyun Park,^{a,b} Jun Hyuck Lee,^{a,b,*}
Ho-Sung Yoon^{c*} and Han-Woo
Kim^{a*}

^aDivision of Polar Life Sciences, Korea Polar
Research Institute, Incheon 406-840, Republic
of Korea, ^bDepartment of Polar Sciences,
Korea University of Science and Technology,
Incheon 406-840, Republic of Korea, and
^cDepartment of Biology, Kyungpook National
University, Daegu 702-701, Republic of Korea

† These authors contributed equally to this
work.

Correspondence e-mail:
junhyucklee@kopri.re.kr, hsy@knu.ac.kr,
hwkim@kopri.re.kr

Received 13 May 2014
Accepted 8 July 2014



© 2014 International Union of Crystallography
All rights reserved

Monodehydroascorbate reductase (MDHAR; EC 1.6.5.4) is a key enzyme in the reactive oxygen species (ROS) detoxification system of plants. The participation of MDHAR in ascorbate (AsA) recycling in the ascorbate–glutathione cycle is important in the acquired tolerance of crop plants to abiotic environmental stresses. Thus, MDHAR represents a strategic target protein for the improvement of crop yields. Although physiological studies have intensively characterized MDHAR, a structure-based functional analysis is not available. Here, a cytosolic MDHAR (OsMDHAR) derived from *Oryza sativa* L. *japonica* was expressed using *Escherichia coli* strain NiCo21 (DE3) and purified. The purified OsMDHAR showed specific enzyme activity (approximately 380 U per milligram of protein) and was crystallized using the hanging-drop vapour-diffusion method at pH 8.0 and 298 K. The crystal diffracted to 1.9 Å resolution and contained one molecule in the asymmetric unit (the Matthews coefficient V_M is 1.98 Å³ Da⁻¹, corresponding to a solvent content of 38.06%) in space group $P4_12_12$ with unit-cell parameters $a = b = 81.89$, $c = 120.4$ Å. The phase of the OsMDHAR structure was resolved by the molecular-replacement method using a ferredoxin reductase from *Acidovorax* sp. strain KKS102 (PDB entry 4h4q) as a model.

1. Introduction

Excess accumulation of reactive oxygen species (ROS) has been recognized as a major factor that causes decreased crop production (Gill & Tuteja, 2010). ROS is generated during metabolic processes or by abiotic stresses such as ozone, drought, flooding, high salinity, heavy metals and extreme temperatures. ROS potentially interact with various cellular molecules and metabolites, resulting in low plant productivity (Apel & Hirt, 2004; Møller, 2001). The intrinsic tolerance of transgenic plants to environmental stresses is increased by the overexpression of various antioxidative enzymes, including superoxide dismutase (SOD), dehydroascorbate reductase (DHAR), ascorbate peroxidase (APX), glutathione reductase (GR) and catalase (CAT) (Sato *et al.*, 2011; Herbette *et al.*, 2011; Allen *et al.*, 1997; Lee *et al.*, 2007; Foyer *et al.*, 1994).

To overcome ROS-induced oxidative conditions, plant cells have developed various protective mechanisms that involve the activation of antioxidant molecules [ascorbate (AsA), glutathione (GSH), α -tocopherol and flavonoids] and antioxidant enzymes [GR, SOD, APX, CAT, DHAR, monodehydroascorbate reductase (MDHAR), glutathione peroxidase (GPX), peroxiredoxin (PRX) and thio-redoxin (TRX) systems] (Mittler, 2002; Allen *et al.*, 1997; Reddy *et al.*, 2004; Inzé & Montagu, 1995; Saruyama & Tanida, 1995; Shao *et al.*, 2008). Among these cell-rescue systems, one prime mechanism involves vitamin C (ascorbate; AsA), which is directly involved in collagen synthesis and several other metabolic processes. AsA also removes radicals generated by aqueous peroxidation, which prevents the peroxidation of membrane lipids. In addition, AsA acts as a substrate in the AsA–GSH pathway of plants and participates in the elimination of ROS, in which it is oxidized to monodehydroascorbate (MDHA) and dehydroascorbate (DHA). To effectively maintain an AsA pool, plants utilize a mechanism for reducing MDHA to AsA which involves the enzyme monodehydroascorbate reductase (MDHAR; Fig. 1; Asada, 1997).

The overexpression of DHAR has been intensively studied in transgenic plants, which exhibit increased adaptation or tolerance to abiotic stresses. In tobacco and rice, the overexpression of DHAR enhances stress tolerance to ozone, high salinity, drought and low temperature by improving redox homeostasis (Eltayeb *et al.*, 2007; Sultana *et al.*, 2012; Eltelib *et al.*, 2011). In addition, DHAR has been reported to light-dependently regulate the AsA pool in tomato (Stevens *et al.*, 2008; Gest *et al.*, 2013). However, information about how DHAR is related to MDHAR overexpression and the plant stress response remains limited. Furthermore, details of the catalytic mechanism at the molecular level have yet to be determined.

In this study, we expressed and purified a cytosolic MDHAR derived from *Oryza sativa* L. *japonica* (OsMDHAR) using an *Escherichia coli* expression system and confirmed the functional activity of OsMDHAR by an enzymatic assay. Preliminary X-ray crystallographic studies were also conducted. This work is the first report of the crystallization and preliminary X-ray diffraction of MDHAR from a higher plant. This information is expected to be valuable for elucidating the stress-tolerance mechanism of plants and for protein engineering to improve this activity.

2. Materials and methods

2.1. Cloning, expression and purification of OsMDHAR

Total RNA was isolated from the leaves of *O. sativa* using an RNeasy Plant Mini Kit (Qiagen, Hilden, Germany). The cDNA was synthesized using an RT-PCR Premix Kit (Bioneer, Daejeon, Republic of Korea) according to the manufacturer's instructions. OsMDHAR (GenBank BAA77214.1) was amplified from cDNA by PCR using *ExTaq* polymerase (Takara Bio Inc., Tokyo, Japan) with forward (5'-GCGGCAGCCATGGCGTCGGAGAAGCACTTCAAG-3') and reverse (5'-GTAGTAGGATCCTTCTTTATTCAAATCTCAGCAGC-3') primers. *Nco*I and *Bam*HI sites are underlined. The amplified PCR products were integrated into the multi-cloning site (MCS) of the pKM260 vector (Euroscarf, Frankfurt, Germany). The final construct was verified by DNA sequencing and was then transformed into *E. coli* strain NiCo21 (DE3) for protein expression (Table 1). The cells were grown in Luria-Bertani (LB) medium at 310 K with 100 µg ml⁻¹ ampicillin until the OD₆₀₀ approached 0.4. The recombinant protein was then induced using 0.2 mM isopropyl

Table 1
Macromolecule-production information.

| | |
|---|--|
| Source organism | <i>O. sativa</i> L. <i>japonica</i> |
| DNA source | mRNA (GenBank BAA77214.1) |
| Forward primer† | 5'-GCGGCAGCCATGGCGTCGGAGAAGCACTTCAAG-3' |
| Reverse primer‡ | 5'-GTAGTAGGATCCTTCTTTATTCAAATCTCAGCAGC-3' |
| Cloning vector | pKM260 |
| Expression vector | pKM260 |
| Expression host | <i>E. coli</i> NiCo21 (DE3) |
| Complete amino-acid sequence of the construct produced§ | MHHHHHASENLYFQGAMASEKHFKYVILGGVVAAGYAAREF-AKQGVKPGELATISKEAVAPYERPALSKGYLFPQNAARLP-GFHVCGSGGERLLPEWYSEKGIELILSTEIVKADLASKT-LTSAVGATFTYEILIIATGSSVIKLSDFGTQGADSNILY-LREVDADKLVAAIQAKKGGKAVIVGGYIGLELSAALKI-NDFDVTMVFPEPWCMPRLFTADIAAFYESYTNKGVKIVK-GTVAVGFDADANGDVTAVNLKNGSVLEADIVGVGGRPL-TTLFKGQVAEEKGGIKTDAFFETSVPGVYAVGDVATPFMK-MYNELRRVEHVDHARKSAEQAVKAIKKGESGESVVEYDYL-PYFYSRFDLQWQFYGDNDVGTTLFGDSDPPTSAKPKFGSY-WIKDGVKLVAFLEGGSDPENKAIKAVKTQPPVANIEELK-KEGLQFASKI |

† The *Nco*I site is underlined. ‡ The *Bam*HI site is underlined. § The His tag and TEV protease cleavage site are underlined.

β-D-1-thiogalactopyranoside (IPTG) at 295 K for 20 h. After induction, the cells were harvested by centrifugation (Centrifuge 5810 R; Eppendorf, Hamburg, Germany) at 4000 rev min⁻¹ and 277 K for 20 min from 4 l culture and were resuspended in cold lysis buffer (50 mM sodium phosphate pH 8.0, 300 mM NaCl, 10 mM imidazole) with 1 mg lysozyme per gram of wet cell pellet, 1 mM phenylmethylsulfonyl fluoride (PMSF) and EDTA-free protease-inhibitor cocktail (PIC; Roche, Mannheim, Germany). After incubation for 30 min on ice, the cells were disrupted by ultrasonication using a short pulse (10 s) with pauses (10 s) for 1 h (Sonic Dismembrator 550; Fisher Scientific Inc., Pittsburgh, USA) on ice. The lysate was centrifuged again to remove cell debris at 16 000 rev min⁻¹ for 30 min at 277 K and the lysate was then poured into a gravity-flow column pre-packed with Ni-NTA resin (Qiagen, Hilden, Germany) that had been pre-equilibrated with the lysis buffer. The bound protein was washed twice with ten column volumes of wash buffer (50 mM sodium phosphate pH 8.0, 300 mM NaCl, 20 mM imidazole) and eluted with elution buffer (50 mM sodium phosphate pH 8.0, 300 mM NaCl, 250 mM imidazole). The OsMDHAR protein was desalted using cold 20 mM Tris-HCl pH 8.0 and concentrated using Amicon Ultra Centrifugal Filters (Ultracel-30K; Merck Millipore, Tullagreen,

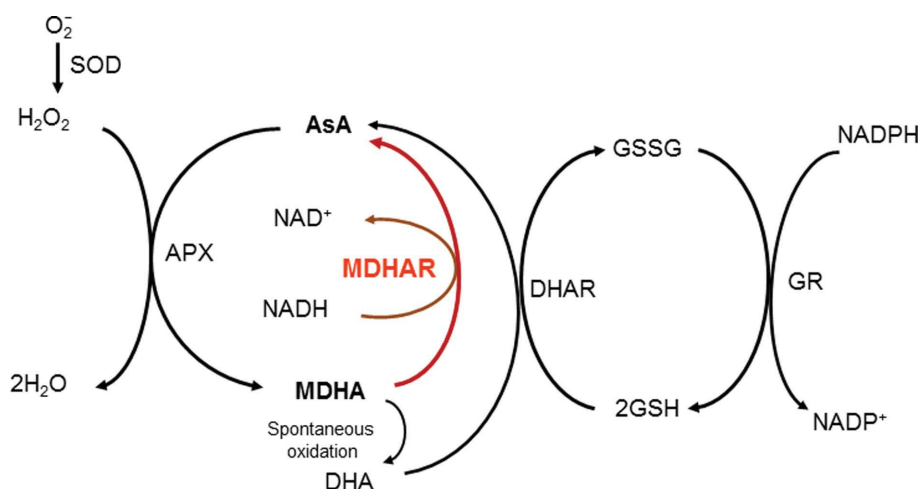


Figure 1
Schematic of MDHAR in the ascorbate–glutathione cycle of plants. SOD, superoxide dismutase; APX, ascorbate peroxidase; MDHAR, monodehydroascorbate reductase; DHAR, dehydroascorbate reductase; GR, glutathione reductase; AsA, ascorbate; MDHA, monodehydroascorbate; DHA, dehydroascorbate; GSSG, oxidized form of glutathione; GSH, reduced form of glutathione.

Ireland) according to the manufacturer's instructions. The resulting protein was concentrated to 15 mg ml⁻¹ for crystallization trials. Protein concentrations were determined spectrophotometrically at 595 nm using Protein Dye Reagent (Bio-Rad, Hercules, USA). The protein samples were stored at 203 K prior to use.

2.2. Protein identification

After SDS-PAGE, the gel was stained with Coomassie Brilliant Blue R-250 (Sigma, St Louis, USA) and then destained. A single band corresponding to the target protein was excised from the gel and subjected to in-gel digestion and matrix-assisted laser desorption/ionization time-of-flight mass spectrometry (MALDI-TOF). Protein identification was performed using *Mascot* (<http://www.matrixscience.com>). The occurrence of a degraded protein species was assessed based on the simultaneous occurrence of the following events: protein identification (estimated *Z* score of >1.6) and an evident discrepancy with respect to the expected molecular mass of the intact protein (a difference of >30%).

2.3. Enzymatic activity of OsMDHAR

The enzymatic activity of the purified OsMDHAR protein was measured spectrophotometrically by quantifying the oxidation of NADH using a previously reported protocol with some modifications (Hossain *et al.*, 1984). The reaction mixture consisted of 50 mM sodium phosphate pH 7.2, 0.2 mM NADH, 2 mM ascorbate, 1 U

ascorbate oxidase (AO) from *Cucurbita* sp. (Sigma-Aldrich, St Louis, USA) and 6.2 µg OsMDHAR protein in a final volume of 1 ml. The enzyme AO was used for the oxidation of ascorbate to produce monohydroascorbate (MDHA). The absorbance was measured at 340 nm. The activity was calculated using an absorbance coefficient of 6.2 mM⁻¹ cm⁻¹. One unit represents the amount of enzyme that oxidizes 1 nmol NADH per minute at 298 K. Bovine serum albumin (BSA; 0.1 mM) was used as a negative control. Enzyme-activity experiments were carried out three or more times and the results are expressed as the mean ± the standard deviation (SD).

2.4. Crystallization and data collection of OsMDHAR

Initial crystallization conditions were screened in MRC 96-well crystallization plates using commercially available screening kits [Wizard Classic 1–4 (Emerald Bio, Seattle, USA), MCSG-1–4 (Microlytic, Burlington, USA) and The Classics and Classics II Suites (Qiagen, Hilden, Germany)]. 0.8 µl protein solution (10 mg ml⁻¹) was mixed with the same volume of reservoir solution and crystallization was carried out by the sitting-drop vapour-diffusion method at 298 K against 80 µl reservoir solution. Initial crystals were observed in a crystallization condition consisting of 100 mM Tris-HCl pH 8.0, 200 mM lithium sulfate, 30% (w/v) PEG 5000 MME. The condition was scaled up using the hanging-drop vapour-diffusion method in a 24-well plate. The volume of the drop was increased from 0.8 to 1 µl and was equilibrated against 500 µl reservoir solution.

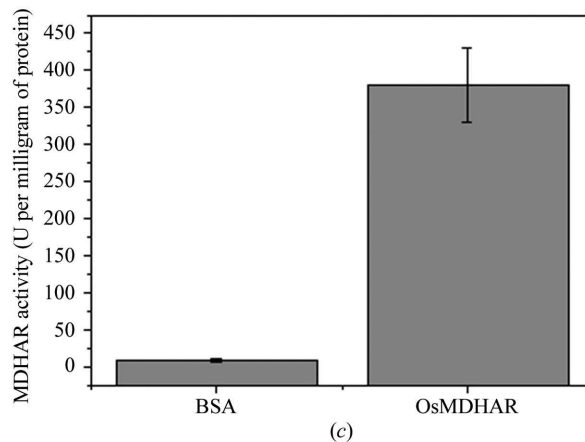
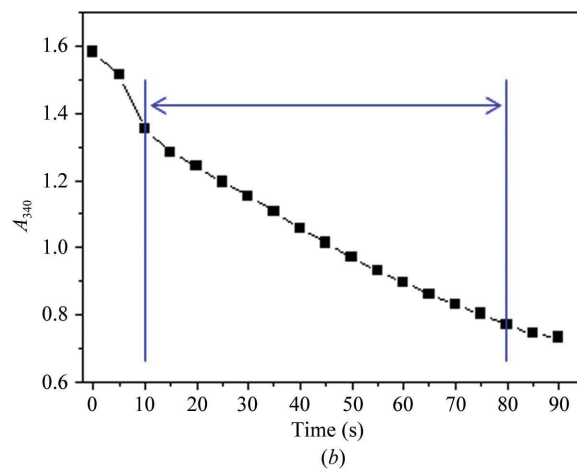
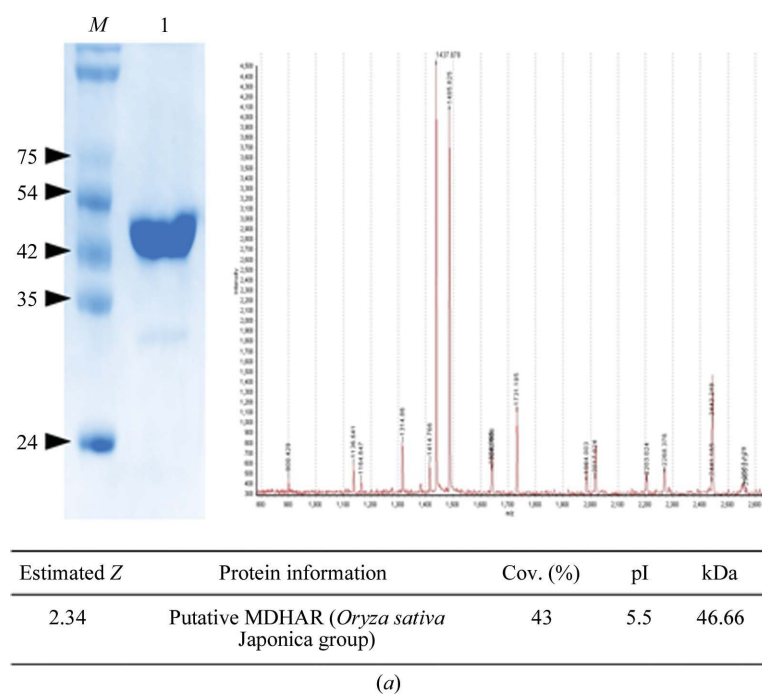
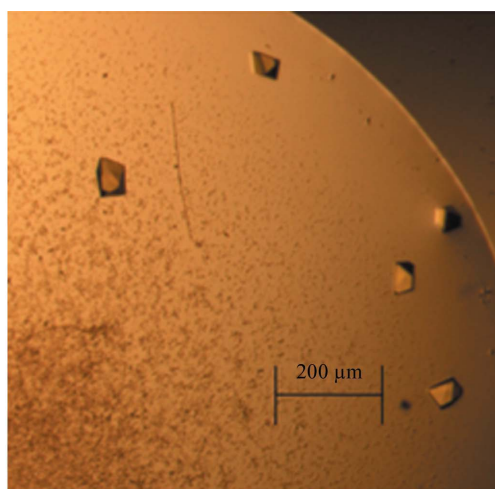


Figure 2 Identification and enzyme activity of the recombinant OsMDHAR protein. (a) Protein identification by MALDI-TOF analysis following SDS-PAGE. (b) Time course of absorbance distribution by NADH oxidation. Bidirectional arrows represent the region used for measuring enzyme activity. (c) Specific enzyme activity of recombinant OsMDHAR. BSA was used as a negative control.

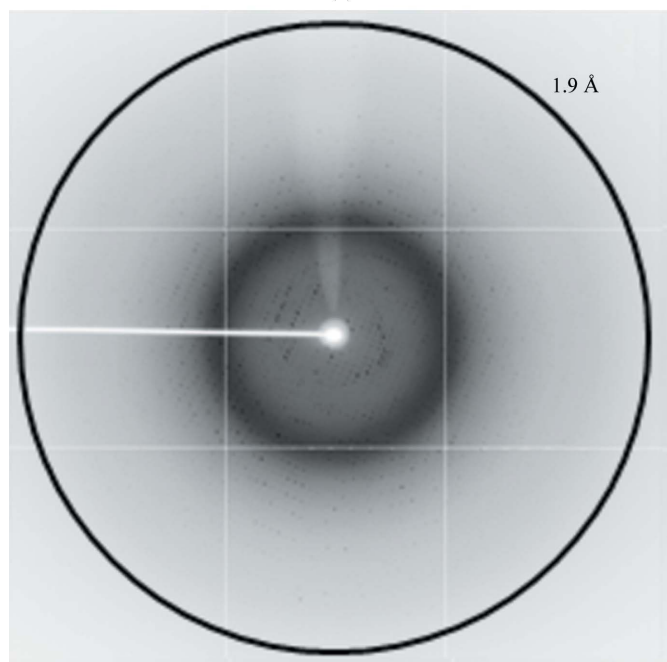
Table 2
Crystallization.

| | |
|--|--|
| Method | Hanging drop |
| Plate type | 24-well plate |
| Temperature (K) | 298 |
| Protein concentration (mg ml ⁻¹) | 10 |
| Buffer composition of protein solution | 10 mM Tris-HCl pH 8.0 |
| Composition of reservoir solution | 100 mM Tris-HCl pH 8.0, 200 mM lithium sulfate, 30% (w/v) PEG 5000 MME |
| Volume and ratio of drop | 1 µl, 1:1 |
| Volume of reservoir (µl) | 500 |

Cube-shaped crystals grew to maximum dimensions of $0.05 \times 0.05 \times 0.05$ mm after 3 d at 298 K under the stated conditions (Table 2). The crystals were introduced into Paratone N as a cryoprotectant and were flash-cooled in a stream of liquid nitrogen at 100 K for X-ray diffraction. A complete data set was collected to 1.9 Å resolution with 1° oscillation, 1 s exposure and a 260 mm crystal-to-detector distance



(a)



(b)

Figure 3

Crystallographic study of OsMDHAR. (a) Morphology of OsMDHAR crystals grown by the hanging-drop method. Their approximate dimensions were $0.05 \times 0.05 \times 0.05$ mm with a cubic shape. (b) Diffraction image of an OsMDHAR crystal.

Table 3

Data collection and processing.

Values in parentheses are for the outer shell.

| | |
|---|---|
| Data collection | OsMDHAR |
| Diffraction source | BL-5C, PAL |
| Wavelength (Å) | 0.97954 |
| Temperature (K) | 100 |
| Detector | ADSC Q315r |
| Crystal-to-detector distance (mm) | 260 |
| Rotation range per image (°) | 1 |
| Total rotation range (°) | 200 |
| Exposure time per image (s) | 1 |
| Space group | $P4_1 2_1 2$ |
| Unit-cell parameters (Å, °) | $a = b = 81.89$, $c = 120.4$, $\alpha, \beta, \gamma = 90$ |
| Mosaicity (°) | 0.41 |
| Resolution range (Å) | 48.64–1.90 (2.00–1.90) |
| Total No. of reflections | 492252 (71239) |
| No. of unique reflections | 33187 (4751) |
| Completeness (%) | 99.9 (100.0) |
| Multiplicity | 14.8 (15.0) |
| $\langle I/\sigma(I) \rangle$ | 16.7 (7.4) |
| $R_{r.i.m.}^\dagger$ | 0.126 (0.447) |
| Overall B factor from Wilson plot (Å ²) | 19.4 |

$^\dagger R_{r.i.m.} = \sum_{hkl} \{ [N(hkl)/[N(hkl) - 1]]^{1/2} \sum_i |I_i(hkl) - \langle I(hkl) \rangle| / \sum_i I_i(hkl) \}$, where $I_i(hkl)$ is the value of the i th intensity measurement and $\langle I(hkl) \rangle$ is the mean value of all measurements of $I(hkl)$.

on beamline 5C (BL-5C) at Pohang Accelerator Laboratory (PAL), Pohang, Republic of Korea. The resulting images were indexed and integrated using *MOSFLM* (Leslie & Powell, 2007) and scaled using programs from the *CCP4* package (Winn *et al.*, 2011). The experimental and data-processing details are summarized in Table 3.

3. Results and discussion

3.1. Identification and enzyme activity of OsMDHAR

The gene for OsMDHAR was amplified and cloned from the cDNA of *O. sativa* L. *japonica*. OsMDHAR was expressed in *E. coli* strain NiCo21 (DE3) to minimize host-protein contamination by endogenous metal-binding proteins in immobilized metal-affinity chromatography. The recombinant protein was successfully purified by Ni-NTA purification. Further purification was performed by analytical size-exclusion chromatography after the addition of nicotinamide adenine dinucleotide hydrate (NADH), the cofactor of MDHAR. The purity of the recombinant protein was about 95% based on SDS-PAGE analysis using a Gel Doc image system (Fig. 2a, upper left panel). The purified protein was identified by MALDI-TOF analysis (Fig. 2a, upper right panel). The isoelectric point (pI) and molecular weight of OsMDHAR were 5.5 and 46.66 kDa, respectively (Fig. 2a, lower panel). Subsequently, the protein was used for experiments to study the enzyme activity and for crystallography. To measure the enzyme activity of OsMDHAR, spectrophotometric analysis was used with commercially available chemical components. As shown in Fig. 2(b), oxidation of NADH was initiated by adding ascorbate oxidase to generate MDHA from AsA. This protein showed significant reductase activity (approximately 380 U per milligram of protein) at pH 7.2 (Fig. 2c). These results indicate that the recombinant OsMDHAR exists in a fully functional form and is folded properly prior to crystallization.

3.2. Crystallization, X-ray diffraction analysis and phase determination

Initial crystals of OsMDHAR were obtained from various conditions after 3 d. The initial crystallization conditions included (i)

100 mM Tris-HCl pH 8.5, 200 mM magnesium chloride, 20% (w/v) PEG 8000, (ii) 200 mM magnesium formate, 20% (w/v) PEG 3350, (iii) 100 mM PCB buffer pH 7.0, 25% (w/v) PEG 1500, (iv) 100 mM Tris-HCl pH 8.5, 200 mM lithium sulfate, 30% (w/v) PEG 4000, (v) 100 mM Tris-HCl pH 8.0, 200 mM lithium sulfate, 30% (w/v) PEG 5000 MME and (vi) 100 mM MES/sodium hydroxide pH 5.5, 200 mM ammonium sulfate, 30% (w/v) PEG 5000 MME.

As a consequence of refinement of initial screening, the best crystals of OsMDHAR were obtained by crystallization with a buffer consisting of 100 mM Tris-HCl pH 8.0, 200 mM lithium sulfate, 30% (w/v) PEG 5000 MME with dimensions of $0.05 \times 0.05 \times 0.05$ mm (Fig. 3a). Data collection was carried out on BL-5C at PAL at a wavelength of 0.97954 \AA using an ADSC Q315r detector. The diffraction data set consisted of 200 frames of data collected to a resolution of 1.9 \AA (Fig. 3b) in 1° oscillation steps with 1 s exposure per frame. The OsMDHAR crystal belonged to space group $P4_12_12$, with unit-cell parameters $a = b = 81.89$, $c = 120.4 \text{ \AA}$ (Table 3). The images were indexed, integrated and scaled using *MOSFLM* and *SCALA* from the *CCP4* package (Leslie & Powell, 2007; Evans, 2006; Winn *et al.*, 2011). A sequence-homology search was performed using the *BLAST* server (<http://www.ncbi.nlm.nih.gov>) at the PDB to search for a model for molecular-replacement calculation. The *BLAST* search results identified the ferredoxin reductase BphA4 (PDB entry 4h4q; Akito *et al.*, 2014) as having the highest sequence similarity. After several molecular-replacement trials, we could only obtain the phase of OsMDHAR by using trimmed coordinates of ferredoxin reductase BphA4 (PDB entry 4h4q), which has 28% sequence identity, in *MOLREP* (Vagin & Teplyakov, 2010). The contrast value of the initial coordinates in space group $P4_12_12$ from *MOLREP* was 3.65 and the *R* factor was 49%. Manual rebuilding using *Coot* (Emsley *et al.*, 2010) and iterative rounds of *REFMAC5* (Murshudov *et al.*, 2011) refinement resulted in reasonable R_{work} and R_{free} values of 20.2 and 25.6%, respectively. During the refinement, 5% of the total reflections were set aside for calculation of the R_{free} value. The presence of a monomer in the asymmetric unit corresponded to a Matthews coefficient of $1.98 \text{ \AA}^3 \text{ Da}^{-1}$ and a solvent content of 38.06% (Matthews, 1968).

We thank the staff at the X-ray core facility of the Korea Basic Science Institute (KBSI), Ochang, Republic of Korea and BL-5C of the Pohang Accelerator Laboratory for their assistance with data collection. This work was supported by the Antarctic Organisms Cold-Adaptation Mechanisms and its application grant (PE14070) funded by the Korea Polar Research Institute, Kyungpook National University Research Fund (2012) and a grant from the Next

Generation BioGreen 21 Program (No. PJ008115012014, Rural Development Administration, Republic of Korea).

References

- Akito, N., Ayaka, H., Miki, S., Yuka, T., Daisuke, M., Shinya, K., Shigemasa, M., Keisuke, S., Toshiya, S. & Shigenobu, K. (2014). *Biochem. J.*, doi:10.1042/BJ20140384.
- Allen, R. D., Webb, R. P. & Schake, S. A. (1997). *Free Radic. Biol. Med.* **23**, 473–479.
- Apel, K. & Hirt, H. (2004). *Annu. Rev. Plant Biol.* **55**, 373–399.
- Asada, K. (1997). *Cold Spring Harb. Monogr. Arch.* **34**, 715–735.
- Eltayeb, A. E., Kawano, N., Badawi, G. H., Kaminaka, H., Sanekata, T., Shibahara, T., Inanaga, S. & Tanaka, K. (2007). *Planta*, **225**, 1255–1264.
- Eltelib, H. A., Badejo, A. A., Fujikawa, Y. & Esaka, M. (2011). *J. Plant Physiol.* **168**, 619–627.
- Emsley, P., Lohkamp, B., Scott, W. G. & Cowtan, K. (2010). *Acta Cryst.* **D66**, 486–501.
- Evans, P. (2006). *Acta Cryst.* **D62**, 72–82.
- Foyer, C. H., Descourvieres, P. & Kunert, K. J. (1994). *Plant Cell Environ.* **17**, 507–523.
- Gest, N., Garchery, C., Gautier, H., Jiménez, A. & Stevens, R. (2013). *Plant Biotechnol. J.* **11**, 344–354.
- Gill, S. S. & Tuteja, N. (2010). *Plant Physiol. Biochem.* **48**, 909–930.
- Herbette, S., de Labrouhe, D. T., Drevet, J. R. & Roedel-Drevet, P. (2011). *Plant Sci.* **180**, 548–553.
- Hossain, M. A., Nakano, Y. & Asada, K. (1984). *Plant Cell Physiol.* **25**, 385–395.
- Inzé, D. & Montagu, M. V. (1995). *Curr. Opin. Biotechnol.* **6**, 153–158.
- Lee, Y.-P., Kim, S.-H., Bang, J.-W., Lee, H.-S., Kwak, S.-S. & Kwon, S.-Y. (2007). *Plant Cell Rep.* **26**, 591–598.
- Leslie, A. G. W. & Powell, H. R. (2007). *Evolving Methods for Macromolecular Crystallography*, edited by R. J. Read & J. L. Sussman, pp. 41–51. Dordrecht: Springer.
- Matthews, B. W. (1968). *J. Mol. Biol.* **33**, 491–497.
- Mittler, R. (2002). *Trends Plant Sci.* **7**, 405–410.
- Møller, I. M. (2001). *Annu. Rev. Plant Biol.* **52**, 561–591.
- Murshudov, G. N., Skubák, P., Lebedev, A. A., Pannu, N. S., Steiner, R. A., Nicholls, R. A., Winn, M. D., Long, F. & Vagin, A. A. (2011). *Acta Cryst.* **D67**, 355–367.
- Reddy, A. R., Chaitanya, K. V. & Vivekanandan, M. (2004). *J. Plant Physiol.* **161**, 1189–1202.
- Saruyama, H. & Tanida, M. (1995). *Plant Sci.* **109**, 105–113.
- Sato, Y., Masuta, Y., Saito, K., Murayama, S. & Ozawa, K. (2011). *Plant Cell Rep.* **30**, 399–406.
- Shao, H.-B., Chu, L.-Y., Lu, Z.-H. & Kang, C.-M. (2008). *Int. J. Biol. Sci.* **4**, 8.
- Stevens, R., Page, D., Gouble, B., Garchery, C., Zamir, D. & Causse, M. (2008). *Plant Cell Environ.* **31**, 1086–1096.
- Sultana, S., Khew, C.-Y., Morshed, M. M., Namasivayam, P., Napis, S. & Ho, C.-L. (2012). *J. Plant Physiol.* **169**, 311–318.
- Vagin, A. & Teplyakov, A. (2010). *Acta Cryst.* **D66**, 22–25.
- Winn, M. D. *et al.* (2011). *Acta Cryst.* **D67**, 235–242.